**J. Life Earth Sci., Vol. 14: 105-121, 2019**
http://banglajol.info.index.php/JLES
**ISSN 1990-4827**


# RETRIEVAL OF BIOMASS BURNING HAZE AEROSOL OPTICAL THICKNESS USING MODIS 500M DATA

**Md. Latifur Rahman Sarker[1*]; Faridzul Adli Zakaria[2]; Janet Nichol[3]; Jeffrey S. Reid[4]; Ahmad Mubin Wahab[5]; Eko Siswanto[6] and Elizabeth A. Reid[4]**

[1]Department of Geography and Environmental Studies, University of Rajshahi, Bangladesh.
[2] Department of Geoinformation, Faculty of Geoinformation and Real Estate, Universiti Teknologi Malaysia, 81310 Johor Bahru, Johor, Malaysia.
[3]Department of Geography, School of Global Studies, University of Sussex, Brighton BN19RH, UK.
[4]Aerosol and Radiation Section, Marine Meteorology Division, Naval Research Laboratory, Monterey CA 93943, USA
[5]Urban and Regional Planning, Faculty of Built Environment, Universiti Teknologi Malaysia, 81310 UTM Johor Bahru, Johor, Malaysia,
[6]Research and Development Center for Global Change (RCGC), Japan Agency for Marine-Earth Science and Technology (JAMSTEC) 3173-25, Showa-machi, Kanazawa-ku, Yokohama, Kanagawa, 236-0001, Japan
[*]Corresponding author's email: lrsarker@ru.ac.bd; lrsarker@yahoo.com

**Abstract:** Recurrent transboundary pollution in Southeast Asia (SEA) from biomass burning poses a severe threat to this region. As a result, there is a need to develop a method for quantifying the aerosol due to biomass burning and their spatial distribution for the enhancement of the current aerosol monitoring techniques in SEA region. Therefore, this study develops an algorithm for the retrieval of biomass burning Haze Aerosol Optical Thickness (HAOT) by incorporating the following elements: i) MODIS 500 m data, ii) a robust radiative transfer code, iii) several combinations of land surface reflectance data, iv) Hybrid Single Particle Lagrangian Integrated Trajectory (HYSPLIT) forward analysis, v) effective cloud masking technique, and vi) image interpolation techniques. The results show strong agreement with the MODIS AOT product ($r^2$ = 0.89–0.93), Aerosol Robotic Network (AERONET) AOT ($r^2$ = 0.80–0.90), Air Pollution Index (API; $r^2$ = 0.80-–0.87), and Pollutant Standards Index (PSI; $r^2$ = 0.90–0.93), which indicates that the proposed algorithm can retrieve HAOT, due to biomass burning, successfully. Although the HAOT algorithm was tested over a limited time from June 19 to June 28, 2013, the robust results suggest that in coordination with point-based measurements, HAOT can be used to improve the detection of aerosol induced haze. However, an adjustment will be necessary if this algorithm is used to retrieve haze aerosol optical thickness induced by biomass burning in different regions.

**Keywords**: haze, Southeast Asia, biomass burning, AOT, API, PSI

**সারাংশ:** দক্ষিণ পূর্ব এশিয়ার (এসইএ) বায়োমাস পোড়ানো থেকে পুনঃসজ্ঘটনশীল আন্তঃসীমান্ত দূষণ এই অঞ্চলের জন্য মারাত্মক হুমকি হয়ে দাঁড়িয়েছে। ফলস্বরূপ, এসইএ অঞ্চলের বায়োমাস পোড়ানোর কারণে সৃষ্ট অ্যারোসোল পরিমান এবং স্থানিক বিস্তারণ পর্যবেক্ষণের বর্তমান কৌশলগুলির উন্নতির জন্য একটি পদ্ধতি তৈরী প্রয়োজন। এ জন্য, এই গবেষণাটি নীচের উপাদানগুলিকে যেমন, ক) মোডিস ৫০০ মিটার তথ্য, খ) উন্নত রেডিয়েটিভ ট্রান্সফার কোড, গ) ভূমি পৃষ্ঠের প্রতিবিম্ব তথ্যের বিভিন্ন সংমিশ্রণ, ঘ) হাইব্রিড সিঙ্গ কণা ল্যাঙ্গরজিয়ান ইন্টিগ্রেটেড ট্র্যাজেক্টোরি (এইচওয়াইএসপিআইএটি) অগ্রবর্তী বিশ্লেষণ, ঙ) কার্যকর ক্লাউড মাস্কিং কৌশল এবং চ) ইমেজ ইন্টারপোলেশন কৌশল সংযুক্ত করে বায়োমাস পোড়ানো থেকে সৃট Haze Aerosol Optical Thickness (HAOT) নির্ধারণের জন্য একটি অ্যালগরিদম তেরী করা হয়েছে। প্রাপ্ত ফলাফল মোডিস এওটি (সহসম্বন্ধ সহজ বর্গ = ০.৮৯-০.৯০) অ্যারোসোল রোবোটিক নেটওয়ার্ক (অ্যারোনট) এওটি (সহসম্বন্ধ সহগ বর্গ = ০.৮০-০.৯০), দূষণকারী স্ট্যাণ্ডর্ড সূচক (পিএসআই) (সহসম্বন্ধ সহগ বর্গ = ০.৯০-০.৯৩) এর সংগে একটি শক্তিশালী সম্পর্ক প্রদর্শন করছে, যা থেকে বোঝা যাচ্ছে যে এই প্রস্তাবিত অ্যালগরিদমটি সফলভাবে বায়োমাস পোড়ানোর কারণে সৃষ্ট অ্যারোসোল পরিমান করতে পারে। যদিও এই অএইআওওটি অ্যালগরিদমটি ১৯৯৯ সালের জুন থেকে ২৮ শে জুন, ২০১৩ পর্যন্ত একটি সীমিত সময়ের মধ্যে পরীক্ষা করা হয়েছে, তবে এই ভালো ফলাফল থেকে প্রতিয়মান যে পয়েন্ট-ভিত্তিক পরিমাপের সাথে সমন্বয় করে এইআওওটি ব্যবহার করলে অ্যারোসোল প্ররোচিত কুয়াশাচ্ছন্নতা সনাক্তকরণ উন্নত হবে। এই অ্যালগরিদমটি যদি ভিন্ন অঞ্চলের বায়োমাস পোড়ানোর দ্বারা সৃষ্ট হ্যাড অ্যারোসোল অপটিক্যাল গভীরতা নির্ধারণে ব্যবহৃত করা হয়, তবে মডেলটিতে কিছু সমন্বয় সাধন প্রয়োজন হবে।

## Introduction

In Southeast Asia (SEA), significant haze episodes from biomass burning in Sumatra and Kalimantan, Indonesia, have occurred almost every one to three years (Chisholm *et al.* 2016). During these events, a thick smoke haze enveloped a large portion of SEA. But notable attention was first drawn at local government and international levels following a severe El Niño-induced haze pollution event in 1997 (Nichol 1998). Many studies have been conducted on the causes and sources of the biomass burning aerosol induced haze event (Nichol 1998) and its effects on human health (Radojevic 1997), air quality (Andreae and Merlet 2001; Mahmud 2009), and climate change (Langmann 2007). However, most previous biomass burning aerosol induced haze monitoring studies largely involve point-based measurements, such as the Malaysian Air Pollution Index (API), Singapore Pollution Standards Index (PSI), and Aerosol Robotic Network (AERONET) aerosol optical thickness (AOT) data. The point-based products can provide high accuracy, but coverage area is small and not available in remote areas where the biomass burning is actually occurring (Lee *et al.* 2006).

In addition to the use of point-based data for aerosol haze monitoring, several remote sensing-based studies have used the MODIS Aerosol Optical Thickness (MODIS AOT) product for determination and characterization of the spatial and temporal distribution of biomass burning haze aerosol (Vadrevu *et al.* 2014; Kaskaoutis *et al.* 2011; Arola *et al.* 2007). MODIS AOT provides high-accuracy over land for global aerosol monitoring owing to its robust retrieval algorithm and effective calibration and cloud screening (Levy *et al.* 2007; Remer *et al.* 2005). However, this AOT product has the following limitations when applied at local and regional levels: i) low spatial resolution of 10 km nadir and up to ~35 km on the swath edge compared with MODIS spectral data of 250 m, 500 m, and 1 km nadir, ii) numerous missing (screened out) pixels (Li *et al.* 2005), iii) larger uncertainties over cloudy regions (Zhang and Reid, 2006), and iv) underestimation of higher aerosol loadings (Remer *et al.* 2005; Wong *et al.* 2010).

Although the global MODIS AOT product has several limitations, it is very much desirable to use satellite data for the monitoring of this recurrent haze in this SEA region since satellite data is freely available over the large and remote areas. But the retrieval process of aerosol optical thickness, that can also be used to determine biomass burning aerosol induced haze, from satellite data is complex (Kaufman *et al.* 1997). The complexity arises due to several factors especially the appropriate selection of a radiative transfer code, retrieval of surface reflectance, and the computation of several atmospheric parameters (Remer *et al.* 2005; Levy *et al.* 2010; Wang *et al.* 2010).

Despite the complexity, several AOT retrieval algorithms have been developed (Kaufman *et al.* 1997; Levy *et al.* 2007) that use different techniques, data, and aerosol/haze pollution phenomena. For example, Li *et al.* (2013) developed a Haze Aerosol Optical Thickness (HAOT) algorithm to estimate haze pollution using MODIS data over the North China Plain based on the assumption that surface reflectance varies little over a short period. Xu *et al.* (2012) also demonstrated the use of MODIS data for monitoring haze pollution over the North China Plain, in which haze distribution was determined by the threshold of apparent reflectance and brightness temperature and Aerosol Optical Depth (AOD) was retrieved by the Deep Blue algorithm (Hsu *et al.* 2006). However, hardly any research has been conducted for the retrieval of haze aerosol optical thickness due to biomass burning in SEA using freely available space born satellite data. Therefore, considering the necessity of the estimation of biomass burning aerosol induced haze aerosol optical thickness and the possibility to develop an algorithm using freely available satellite data, this study proposes an algorithm for the retrieval of haze aerosol optical thickness of biomass burning in SEA using MODIS 500m data.

## Study area and data

### Study area

The basis of development of this algorithm is derived from the significant June 2013 biomass burning aerosol induced haze event that affected wide areas of SEA region, particularly Singapore, Peninsular Malaysia, and the Riau Province of Indonesia (Vadrevu *et al.* 2014) (Fig. 1). Generally this study site is characterized by light westerly winds, particularly during the daytime in inter-monsoonal conditions (Mahmud, 2009), which plays an important role in exacerbating the pollution during haze pollution events (Dominick *et al.* 2012). The southwest monsoon brings cross-equatorial haze pollution from Indonesia to Singapore and Peninsular Malaysia within 12–24 h (Koe *et al.* 2001; Reid *et al.* 2012). Two AERONET stations are available for HAOT validation in Singapore and Penang, Malaysia, respectively. Additionally, 35 API and 5 PSI stations operate in Peninsular Malaysia and Singapore, respectively (Fig. 1).


**Fig. 1** Study area showing AERONET, API, and PSI stations

## Data

The dataset we utilized in this study is based on June 2013 haze pollution event since it was a severe biomass burning aerosol induced haze event in this SEA region. Several types of data were used for the development of the HAOT algorithm and its validation (Table 1). MODIS Terra level 1B calibrated radiances MOD02HKM , MODIS daily (MOD09GA) and weekly (MOD09A) land surface reflectance products, and MODIS geolocation data (MOD03), were used as inputs for the HAOT model development. A few bands (i.e., bands 1, 2, 3, and 6) of MODIS MOD02HKM data were used to generate the cloud mask. Additionally, the cirrus reflectance band 48 of MODIS cloud product MOD06, was used for masking cirrus clouds. Moreover, several other datasets such as MODIS aerosol product (MOD04), AERONET AOT, API, and PSI were used to validate the retrieved HAOT due to biomass burning.

**Table 1** General characteristics of MODIS data used in this study

| Data | Level | Spatial resolution (m) | Band | Primary use |
|---|---|---|---|---|
| MOD02HKM | 1B | 500 | 4 | TOA reflectance |
| | | | 2 | Cloud masking |
| | | | 3 | Cloud masking |
| MOD03 | 1A | 1000 | 2, 3, 5 & 6 | Satellite and solar geometry |
| MOD09GA | 2G | 500 | 4 | Surface reflectance (daily) |
| MOD09A | 2G | 500 | 4 | Surface reflectance (weekly) |
| MOD06 | 2 | 1000 | 48 | Cirrus cloud masking |
| MOD04 | 2 | 10000 | 8 | AOT product for validation |

## Materials and Methods

The retrieval of haze aerosol optical thickness (HAOT) from biomass burning in SEA was carried out by matching two types of top of atmosphere reflectance (ρTOA). The first ρTOA was obtained from MODIS data, hereafter referred to as ρTOA_MODIS. The second ρTOA, hereafter referred to as ρTOA_modeled, was obtained theoretically through the use of the 6SV radiative transfer code based on different levels of AOT loadings as well as atmospheric conditions and the geometries of the satellite and the Sun. A series of sequential processing steps was followed to retrieve HAOT from the MODIS 500 m data. However, the total processing chain of this retrieval process included the following steps: i) pre-processing of satellite data, ii) cloud mask generation, iii) determination of MODIS top of atmosphere reflectance (ρTOA_MODIS), iv) determination of modeled top of atmosphere reflectance (ρTOA_modeled), v) retrieval of haze aerosol optical thickness, vi) validation of the HAOT results, vii) determination of the aerosol induced haze transportation using forward trajectory analysis, and viii) interpolation of HAOT maps for reducing missing pixels problem.

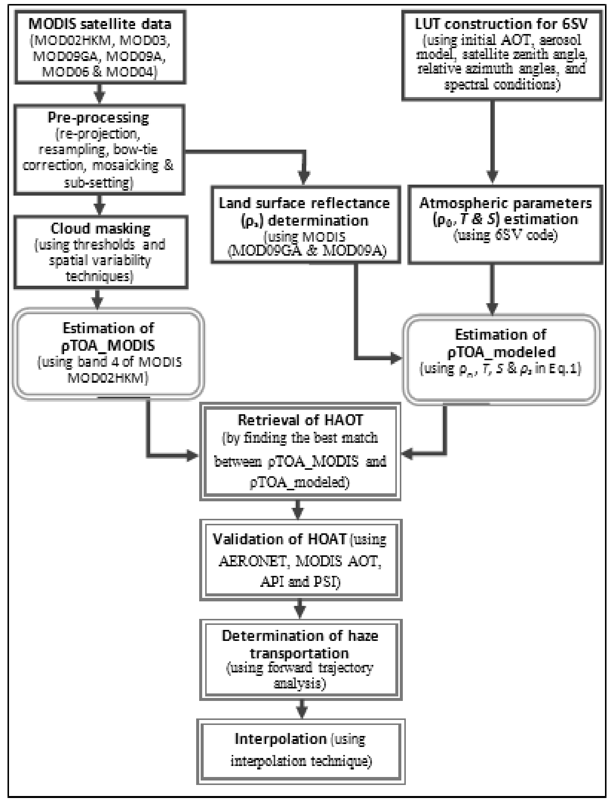


**Fig. 2** Overall work flow

## Pre-processing of satellite data

The pre-processing of MODIS Terra data was conducted by following several sequential steps. First, re-projection was performed for all selected MODIS data (MOD02HKM, MOD03, MOD04, MOD06, and MOD09) by using the MODIS Conversion Tool Kit (MCTK) plug-in for ENVI. The Universal Transverse Mercator (UTM) project (zone 48N) and WGS-84 datum were used as the projection parameters, and the nearest neighbor re-sampling method was used for re-sampling of all data to 500 m. However, bow-tie correction was applied for only MOD02HKM data during the re-projection using MCTK. Image mosaicking was performed when more than one satellite image were used to cover the entire study area. Finally, a sub-setting process was performed by using a region of interest (ROI) mask to focus on the study area only.

**Cloud mask generation**

Of the several uncertainties related to the aerosol optical thickness retrieval process, cloud bias is the most important source of that in SEA, with thin cirrus clouds covering 80% of the sky (Tian *et al.* 2008; Reid *et al.* 2012). Considering the nearly ubiquitous cloud cover in SEA, several types of cloud mask products were tested to separate cloud and biomass burning aerosol induced haze pixels. Unfortunately, this study was unable to find a mask from the available cloud products that can be used for HAOT retrieval without a significant loss of aerosol induced haze pixels. This was happened due to the fact that global cloud products are generated by using a different set of cloud masking and quality control procedures that lead to a very conservative mask (Reid *et al.* 2013), and no consideration is given for local or regional incidents. As a result, a method was adopted for constructing cloud masks based on thresholds and a spatial variability technique that involves only a few steps: i) detecting cloud and aerosol induced haze pixels, ii) masking clear cloud pixels, iii) masking unwanted cirrus cloud pixels, and iv) creating a final cloud mask.

**Determination of MODIS top of atmosphere reflectance (ρTOA_MODIS)**

After pre-processing the necessary satellite data, the first part of the HAOT retrieval involved deriving ρTOA from MODIS level 1B calibrated radiance data (MOD02HKM 500 m). The ρTOA_MODIS was retrieved by normalizing the calibrated radiance of MODIS MOD02HKM of band 4 based on solar illumination following the method of von Hoyningen-Huene *et al.* (2006). However, the necessary parameters for this normalization process such as mean solar exo-atmospheric irradiance for MODIS band 4 and the Earth–Sun distance in astronomical units were obtained from the studies of Chander *et al.* (2010) and Duffie and Beckman (1994), respectively.

**Determination of modeled TOA reflectance (ρTOA_MODIS) using radiative transfer code**

The ρTOA_modeled was computed by using Eq. 1 (Kaufman *et al.* 1997):

$$\rho TOA\_modeled\ (\mu_s,\ \mu_v,\ \varphi) = \rho_0(\mu_s,\ \mu_v,\ \varphi) + \frac{T(\mu_s)T(\mu_v)\rho_S(\mu_s,\mu_v,\varphi)}{[1-\rho_S(\mu_s,\mu_v,\varphi)S]}, \quad \text{(Eq. 1)}$$

where $\rho_0$ is the atmosphere path reflectance, $T$ is the transmission function describing the atmospheric effect on upward and downward reflectance, $S$ is the atmosphere backscattering ratio, and $\rho_s$ is the angular surface reflectance. Three of these parameters, $\rho_0$, $T$, and $S$, are actually functions of the solar zenith angle ($\mu_s$), satellite zenith angle ($\mu_v$), and relative azimuth angle ($\varphi$). Moreover, each term on the right-hand of Eq. 1 is also a function of AOT and aerosol type, except for surface reflectance (Levy *et al.* 2007; Li *et al.* 2013). To determine the $\rho$TOA_modeled, all four terms of Eq. 1 need to be estimated; the processes for estimating these four parameters are discussed in the following two sub-sections.

**Estimation of atmospheric parameters ($\rho_0$, $T$, and $S$) for ρTOA_modeledestimation**

The three atmospheric parameters, i.e., $\rho 0$ (path reflectance), $S$ (backscattering ratio), and $T$ (upward total transmission) in Eq. 1 were estimated using 6SV radiative transfer code developed by Kotchenova *et al.* (2006). The parameters were estimated on a pixel-by-pixel basis, and a look up table (LUT) was created (Table 2) to input the necessary parameters including initial AOT, aerosol model, satellite zenith angle, relative azimuth angles, and spectral conditions into the 6SV radiative transfer code. Simulation for estimating ρTOA_modeled was performed under different initial AOT loading from 0.01 to 5.0 with intervals of 0.1 and 0.01 and for a variety of geometries. However, this study used only the biomass burning aerosol model since the haze pollution induced by the biomass burning aerosol was the main focus of this study. All the parameters $\rho_0$, $T$, and $S$ were calculated using a radiative transfer code by assuming that surface reflectance is zero.

**Table 2** Parameters used for the lookup table (LUT) in the 6SV radiative transfer code

| Name of parameter | Used value |
|---|---|
| Wavelength | 0.550 μm |
| Initial AOT values at 0.550 μm | 0.01–5, Δ = 0.01 and 0.1 |
| Solar zenith angle | Real value for each satellite data point |
| View zenith angle | Real value for each satellite data point |
| Relative azimuth angle | Real value for each satellite data point |
| Atmospheric model | Tropical |
| Aerosol model | Biomass burning |

**Determination of surface reflectance**

Surface reflectance ($\rho_s$), a crucial parameter for estimating pTOA_modeled, can be estimated by using different algorithms. In this study, however, the surface reflectance was obtained from the MODIS land surface reflectance product because it has been validated to have high accuracy through a robust validation process using AOT data from 40 AERONET stations distributed over different land cover types globally (Vermote and Kotchenova, 2008). Nevertheless, considering the importance of surface reflectance, this study investigated the potential of MODIS land surface reflectance for HAOT retrieval using four models. In Model-1, the daily surface reflectance product (MOD09GA) was tested. In Model-2, the weekly (eight-day) land surface reflectance (MOD09A) immediately before the incident of haze was used because weekly surface reflectance is more reliable than daily values. In Model-3, three-week land surface reflectance excluding haze days was used to investigate the averaging effect of land surface reflectance. In Model-4, averaging of the four-week MOD09A product including haze days was used.

**Retrieval of Haze Aerosol Optical Thickness (HAOT)**

The concept behind retrieval of HAOT due to biomass burning using satellite data is to find the closest match between the two types of top of atmospheric reflectance (ρTOA) i.e. i) ρTOA_MODIS (obtained from MODIS data), and ii) ρTOA_modeled (obtained using radiative transfer code). The daily series of ρTOA_modeled reflectance was generated by using Eq. 1 by combining the estimated atmospheric parameters ($\rho_0$, *T,* and *S*) generated from the radiative transfer code based on different levels of AOT and other parameters and the land surface reflectance ($\rho_s$) obtained from the MODIS land surface reflectance product.

To find the best match between ρTOA_MODIS and ρTOA_modeled for each pixel, a technique (Eq. 2) was used to estimate the lowest residual between ρTOA_MODIS and ρTOA_modeled employing an iterative process to search for the best value of the initial AOT:

$$x^2 = \left(\rho TOA\_MODIS - \rho TOA\_modeled_{AOT_{i \dots n}}\right)^2$$
(Eq. 2)

where x is the residual between ρTOA_MODIS and ρTOA_modeled, ρTOA_MODIS = MODIS 500 m TOA reflectance, ρTOA_modeled = modeled TOA reflectance, and $AOT_{i \dots n}$ is the initial AOT, from 0.01 to 5.0 at intervals of 0.1, which was used to generate a specific ρTOA_modeled value.

However, once the closest match between ρTOA_MODIS and ρTOA_modeled was determined for a specific pixel based on the minimum $x^2$ value, the initial corresponding AOT value of ρTOA_modeled was linearly interpolated to the same pixel of ρTOA_MODIS. This iterative process was continued until the best match for all pixels was found and was linearly interpolated. The result is a complete haze aerosol optical thickness (HAOT) map for each day using the MODIS 500 m data.

**Validation of the results**

All of the HAOT retrieval models were validated by using operational MODIS AOT and level 1.5 AERONET AOT data. A comparison of HAOT with API (Malaysia) as well as PSI (Singapore) were conducted to explore the possibility of using the HAOT map as complementary information for API and PSI. For validation, an area of interest (AOI) mask based on single pixel, 2 × 2 pixels, and 3 × 3 pixels were used to extract data from the all HAOT maps over the validation points. Usable pixels were averaged to obtain stable measurements. Moreover, an averaging of AERONET data within ±30 min (Levy *et al.* 2007) of the MODIS overpass time was used, whereas measurements at 12:00 LT were used without averaging for API and PSI. Finally, validation accuracy was assessed by calculating several commonly used statistical parameters such as coefficient of determinant ($r^2$), and root–mean–square error (RMSE).

**Determination haze transportation using forward trajectory analysis**

HYSPLIT (http://ready.arl.noaa.gov/HYSPLIT.php; Dreher 2009) was used to determine the spatial relationship between the retrieved HAOT and the effects of biomass burning aerosol induced haze transportation from its source areas by seasonal winds. Since previous studies indicate that much of the haze pollution for the June 2013 event originated from fires in Riau Province, Indonesia (Vadrevu *et al.* 2014), this study used forward HYSPLIT to simulate biomass burning aerosol induced haze movement by selecting fire hotspots in Riau Province as the source of the pollution. The forward HYSPLIT model was run in 6 h increments (00 h, 06 h, 12 h and 18 h) to track air parcels from the source to their destinations at two different altitudes of 500 m and 1000 m on specific days throughout the total period of the 2013 biomass burning aerosol haze event.

**Interpolation of HAOT maps**

Missing pixels due to cloud cover are a severe problem SEA region (Vadrevu *et al.* 2014), which makes it impossible to obtain a complete scenario of any processing output using optical satellite data. Considering this problem, we used an interpolation technique known as the Penalized Least Squares Method, which is based on discrete cosine transform and nearest-neighbor interpolation (Garcia 2010), to interpolate daily HAOT map for obtaining a daily HAOT map without missing pixels.

## Results

### Results of cloud masking

The first step of cloud masking was performed by identifying the different types of clouds and aerosol induced haze affected areas using the RGB display of MODIS data. Although, this process is not quantitative, it helped to explain the overall scenario of cloud and haze pollution and to determine the general types of clouds that are eliminated by the next two steps. The result from the first step (Fig. 3a) revealed a few features such as clear clouds, mixed clouds, cirrus clouds, and probable aerosol induced haze with or without clouds, as depicted in Fig. 3a as black, orange, yellow, and violet squares, respectively.

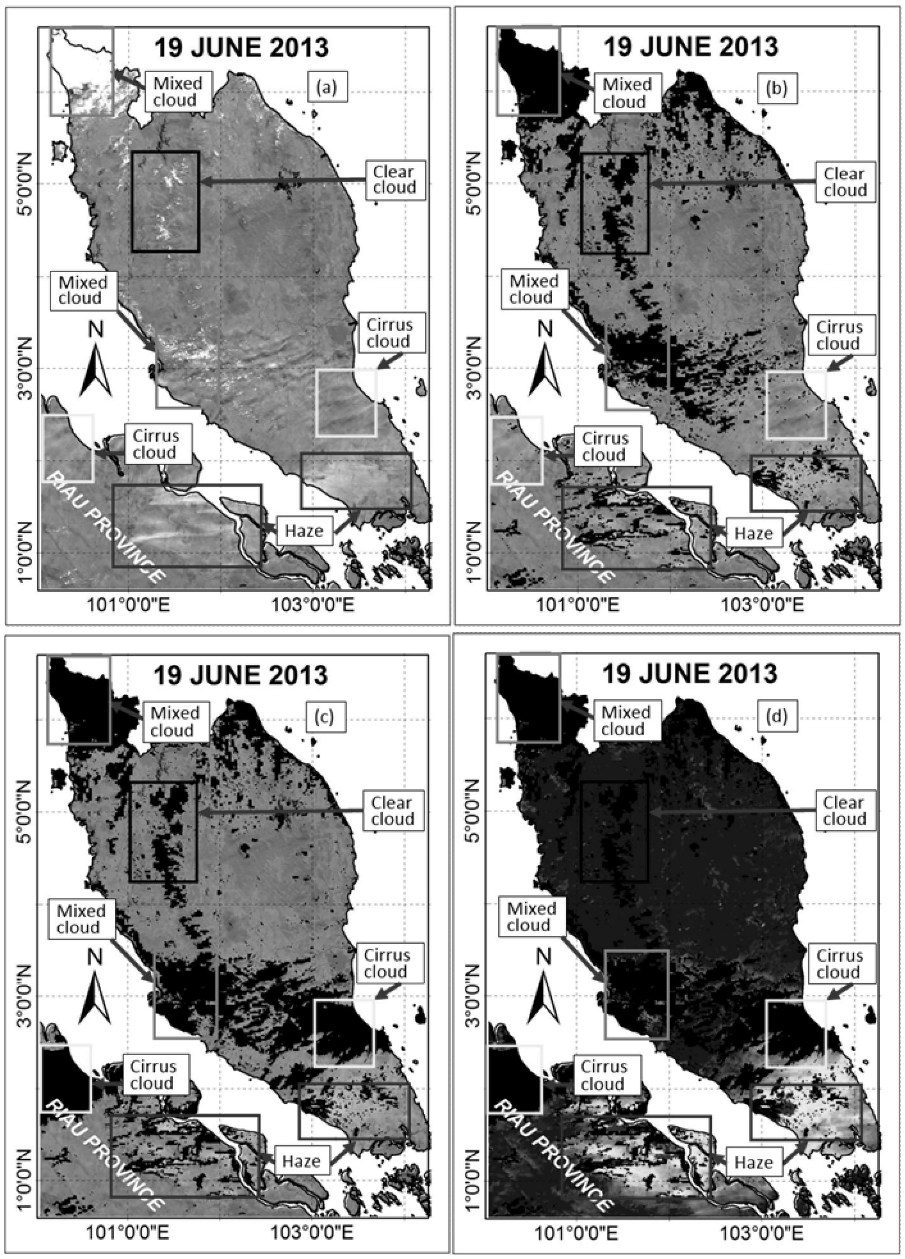


**Fig. 3** Cloud-masking steps: a) detection of different type of clouds; b) masking of clear and mixed clouds; c) masking of cirrus clouds; d) final masking with a sample HAOT map

In the second step, we first generated a cloud mask using the direct thresholding (0.31–0.40) of band 2 of MOD02HKM that effectively eliminated most of the clear cloud pixels. However, an additional mask was constructed from band 3 of MOD02HKM to remove scattered cloud-contaminated pixels by using a spatial variability method in which several thresholds of standard deviation (i.e., from 0.10 to 0.25) were used. It is noticeable from the results (Fig. 3b) that most of the cloudy pixels were removed during the second step of masking, although the cirrus cloud and aerosol induced haze pixels were still present (Fig. 3b).

During the next step, a third mask was generated by using MODIS cirrus reflectance (band 48 of MOD06) by using a thresholding method to remove unwanted few cirrus cloud pixels. The results indicated a successful removal of cirrus cloud pixels without a significant loss of aerosol induced haze pixels (Fig. 3c).

Finally, all three masks were combined and were used to mask out all the cloud contaminated pixels. As a result, we were able to observe the aerosol induced haze-affected areas after applying the created mask to a sample retrieved HAOT map (Fig. 3d). Almost the same process was applied to remove cloud-contaminated pixels from all of the investigated days. However, the selected thresholds for mask generation varied slightly on a daily basis in response to the magnitudes of cloud contamination, and other factors. The result, RGB with all masks and haze transportation trajectories, is presented in Fig. 4. It is evident that while this masking process is effective, it is dependent on the severity of cloud contamination.

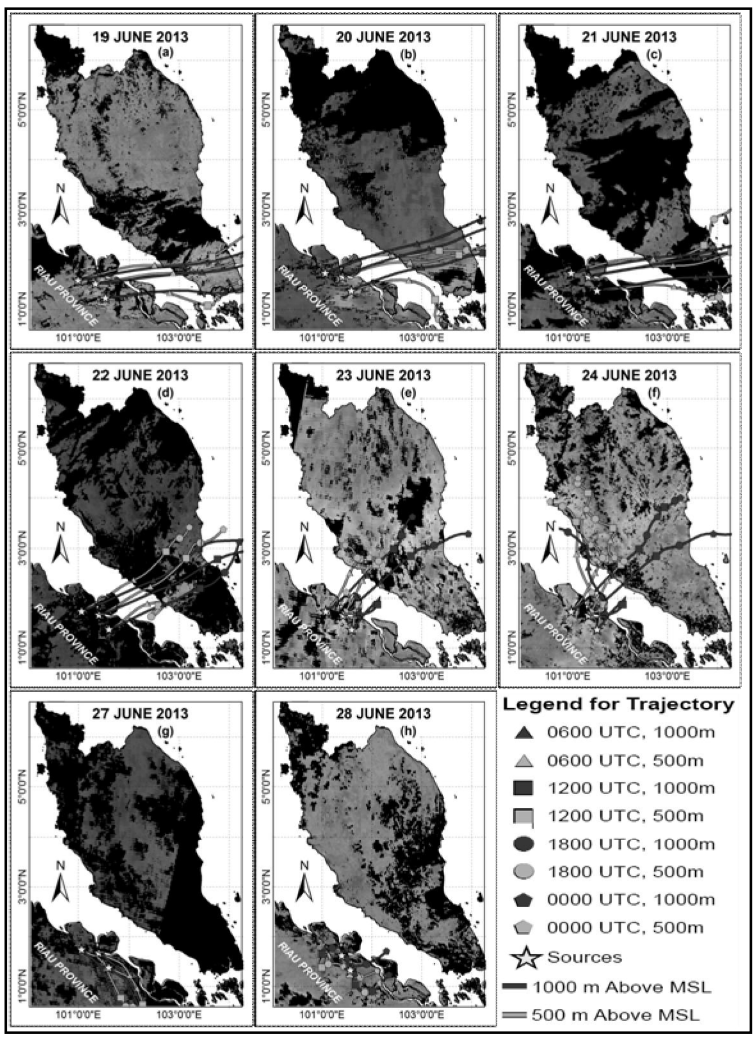


**Fig. 4** Visualization of MODIS RGB after all masks were applied along with the biomass burning aerosol induced haze transportation trajectories

**HAOT model validation and comparison**

Retrieval of HAOT was conducted for several days during the biomass burning aerosol induced haze occurrence from June 19 to 28, 2013, to evaluate the effectiveness of the algorithm. Although biomass burning aerosol induced haze incidents were observed from June 19 to 28, 2013, this study was unable to produce a HAOT map for June 26 and 27 due to severe cloud contamination and missing MODIS data. Four HAOT retrieval models were developed: Model-1, Model-2, Model-3, and Model-4. All models were validated by using the MODIS AOT product (MOD04), AERONET AOT, API, and PSI data. The validation as well as comparison results are presented in the following two sub-sections.

**Validation of HAOT with MODIS AOT**

Validation of the HAOT results with MODIS AOT product (MOD04) was conducted by using data from several paired points from each of the dates, although the number of used points varied owing to missing pixels, especially in MOD04. As shown in Fig. 5, the estimated HAOT correlated strongly with the MODIS AOT product. All four retrieval models were able to effectively estimate HAOT, with the highest accuracy ($r^2$ = 0.93, RMSE = 0.20) obtained by using Model-2 (Fig. 5b) and the lowest ($r^2$ = 0.89, RMSE = 0.24) obtained for Model-1 (Fig. 5a). Model-3 and Model-4 were only slightly inferior to the best model, as shown in Figs. 5c and 5d, respectively. The 4% difference in accuracy between the top and bottom performers is likely attributed to the different types of land surface reflectance (weekly versus daily) used in the computation.

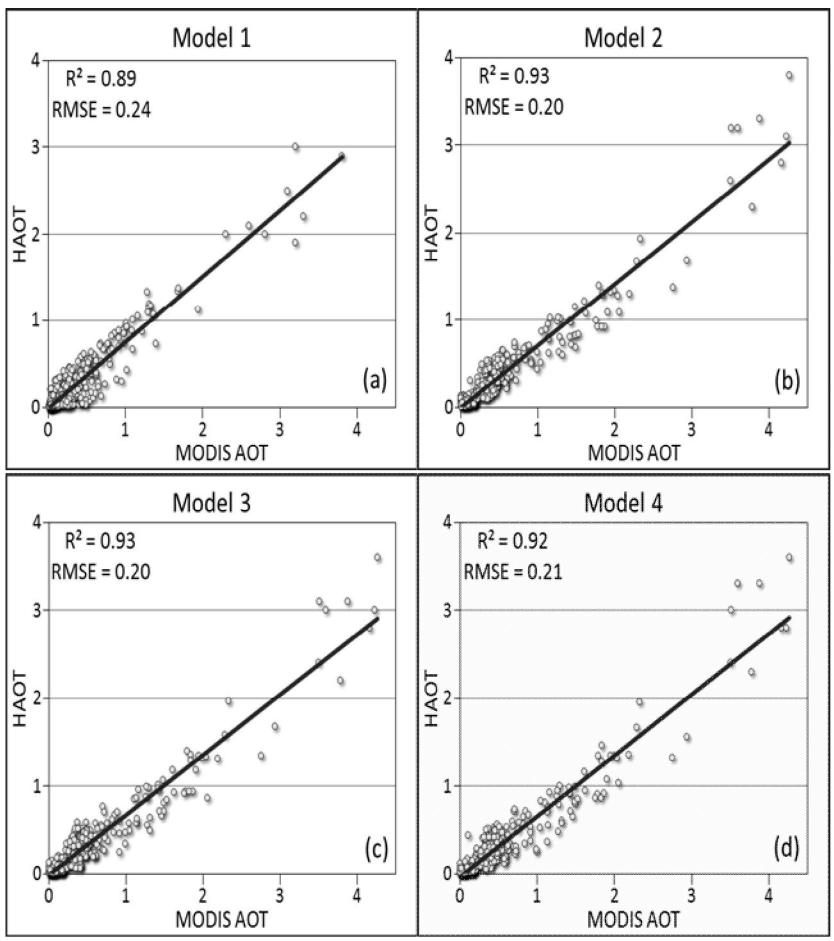


**Fig. 5** Comparison of the MODIS AOT and HAOT retrieved from the proposed algorithm: a) Model-1, which used the daily surface reflectance product; b) Model-2, which used weekly surface reflectance; c) Model-3, which used three-week surface reflectance except for haze days; d) Model-4, which used four-week surface reflectance including haze days

Apart from quantitative assessment, a visual comparison was also made between the operational MODIS AOT product at 10 km (Fig. 6a2 and Fig. 6b2) and the generated HAOT using 500 m MODIS data (Fig. 6a3 and Fig. 6b3) by visual examination; the MODIS RGB images with cloud masks were also used in the comparison (Fig. 6a1 and Fig. 6b1). This assessment (Fig. 6) indicated two observations: i) the spatial distribution of biomass burning aerosol in the HAOT maps (Fig. 6a3 and Fig. 6b3) shows significant improvement over the MODIS AOT maps (Fig. 6a2 and Fig. 6b2), and ii) the problem of missing pixels is more apparent with MODIS AOT than with HAOT generated by this algorithm. These results can be attributed to three factors i.e. i) the differences in spatial resolution of MODIS AOT (10 km) and HAOT (500 m) resulted in fewer pixels in the MODIS AOT maps (Fig. 6a2 and Fig. 6b2) than those in the HAOT maps (Fig. 6a3 and Fig. 6b3) generated by this algorithm, ii) the very aggressive cloud screening process used in the MODIS AOT product generation (Reid *et al.* 2013), and iii) very little to no scope for considering regional or local phenomena for MODIS AOT product generation algorithm.

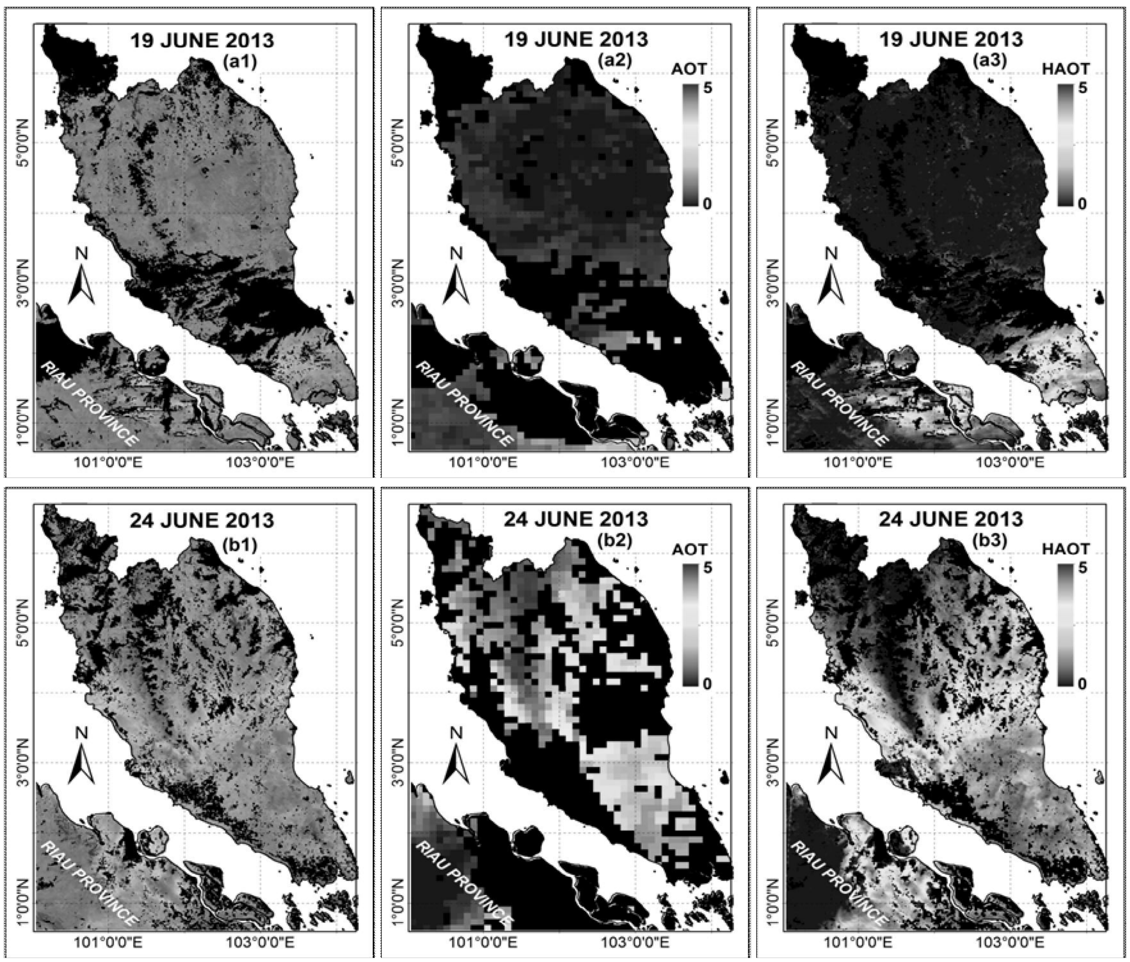


**Fig. 6** Visual comparison of MODIS AOT product and HAOT results

**Validation of HAOT with AERONET AOT data**

For validation using AERONET, although efforts were made to obtain data for all of the dates from the Singapore and USM Malaysia AERONET stations, very few data were usable due to cloud contamination. As shown in Fig. 7, the HAOT correlated strongly with the AERONET AOT. More than 80% accuracy ($r^2 >$ 0.80) was found for all four HAOT retrieval models, although the accuracy varied among them. The lowest accuracy ($r^2 = 0.80$) was obtained using Model-1 (Fig. 7a) which was similar to the validation results against MODIS AOT; the highest accuracy ($r^2 = 0.90$) was obtained from Model-4 (Fig. 7d), which used monthly surface reflectance. However, very similar accuracy

($r^2$ = 0.87) was obtained by using the other two HAOT models (Model-2 and Model-3). Overall, the results suggest that the proposed biomass burning aerosol induced haze retrieval algorithm is effective and that HAOT correlates strongly with ground-based AERONET AOT and the MODIS AOT products.

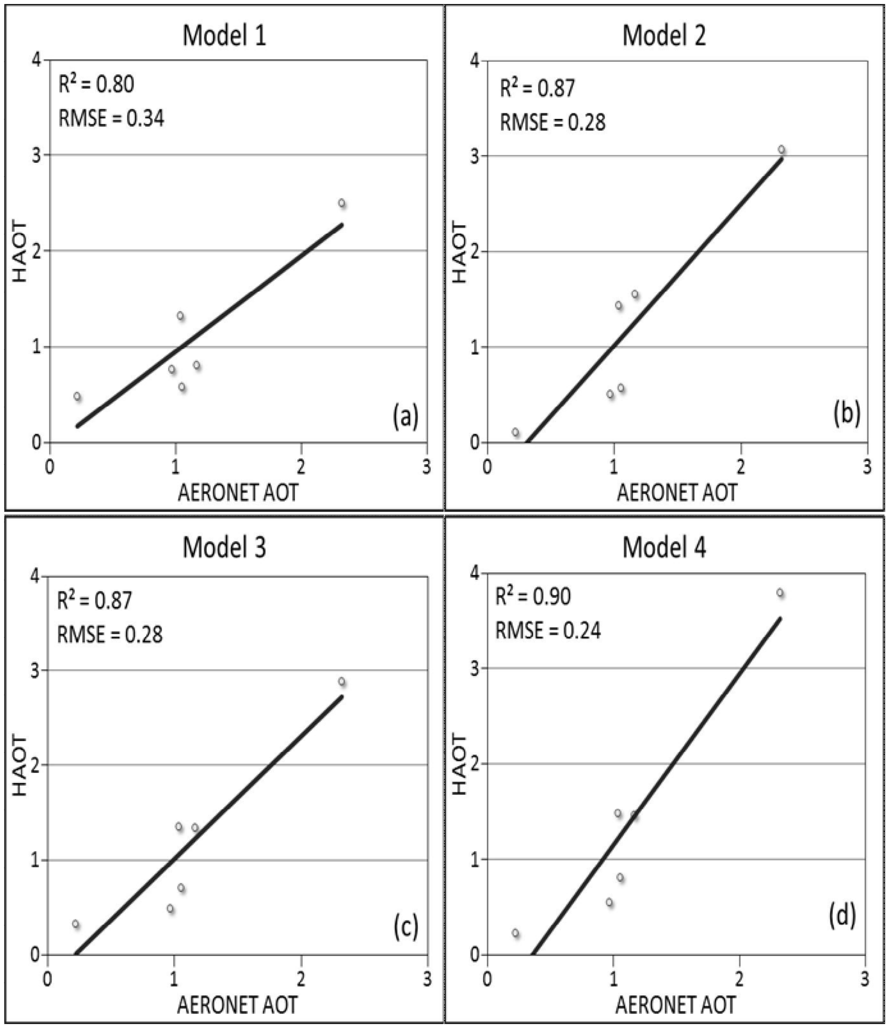


**Fig. 7** Comparison of AERONET AOT and HAOT: a) Model-1, which used the daily surface reflectance product; b) Model-2, which used weekly surface reflectance; c) Model-3, which used monthly surface reflectance excluding haze days; d) Model-4, which used monthly surface reflectance including haze days

**Comparison of HAOT with API and PSI data**

The estimated HAOT was also compared with API and PSI, used in Malaysia and Singapore, respectively, because these ground-based measurements are used as air-quality indicators for the two countries. As shown in Fig. 8, HAOT correlated strongly with API, with all four HAOT models correlating with high accuracy ($r^2$ > 0.80). The highest and lowest accuracies, at $r^2$ = 0.87 and $r^2$ = 0.80, respectively, were achieved by using HAOT retrieval Model-2 (Fig. 8b) and Model-1 (Fig. 8a) respectively, although the accuracies of the other two models (Model-3; Fig. 8c and Model-4; Fig. 8d) were very similar to that of Model-2. For the PSI, the results also indicate that the proposed algorithm was able to retrieve ground-level pollution effectively because the agreement between PSI and HAOT for all four models was very strong. All four models showed correlation of about 90% ($r^2$ = 0.90), and, similar to the comparison between HAOT and API, the highest ($r^2$ = 0.93) and lowest ($r^2$ = 0.90) correlations were also obtained by using Model-2 (Fig. 9b) and Model-1 (Fig. 9a) respectively.

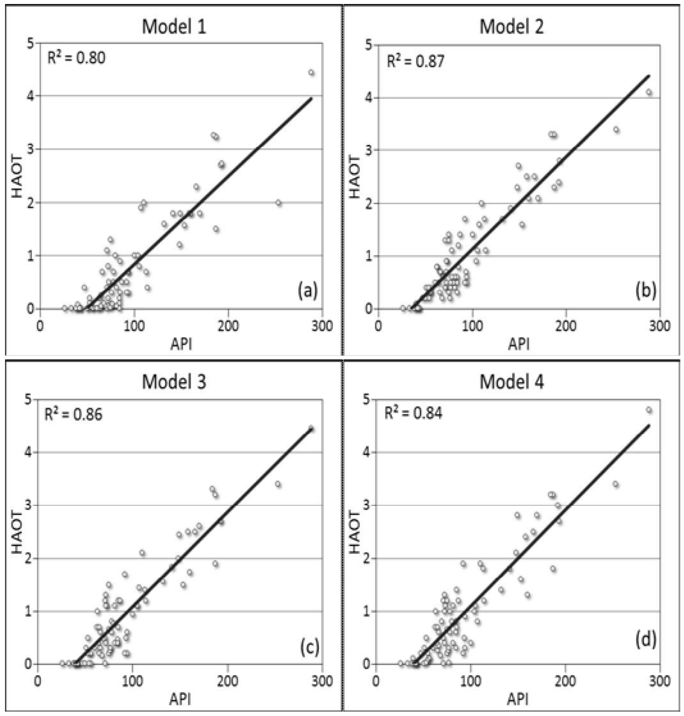


**Fig. 8** Comparison of API and HAOT: a) Model-1, which used the daily surface reflectance product; b) Model-2, which used weekly surface reflectance; c) Model-3, which used monthly surface reflectance excluding haze days; d) Model-4, which used monthly surface reflectance including haze days

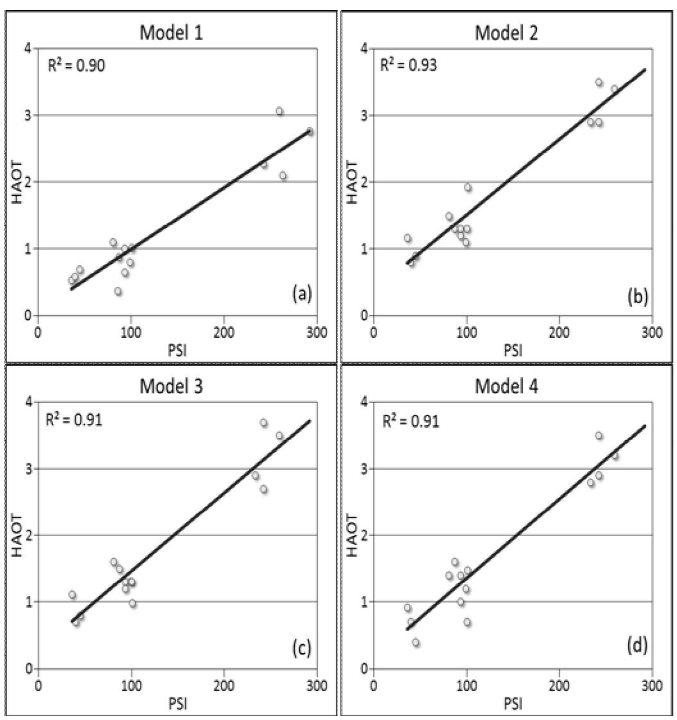


**Fig. 9** Comparison of PSI and HAOT: a) Model-1, which used the daily surface reflectance product; b) Model-2, which used weekly surface reflectance; c) Model-3, which used monthly surface reflectance excluding haze days; d) Model-4, which used monthly surface reflectance including haze days

**Spatial and temporal distribution of retrieved HAOT using the selected algorithm (Model-2)**

The results from all four proposed HAOT retrieval models were favorable, although the accuracy varied. The lowest $r^2$ and RMSE was reported for Model-1, which used daily surface reflectance. The performances of Model-2, Model-3, and Model-4, developed using weekly, three-week, and four-week land surface reflectance, respectively, were similar; however Model-2 showed slightly better performance than the other two models in some of the validation processes. Therefore, in this section, we present the spatial distribution of the retrieved haze aerosol optical thickness using the results of only Model-2 along with the haze transportation trajectories.

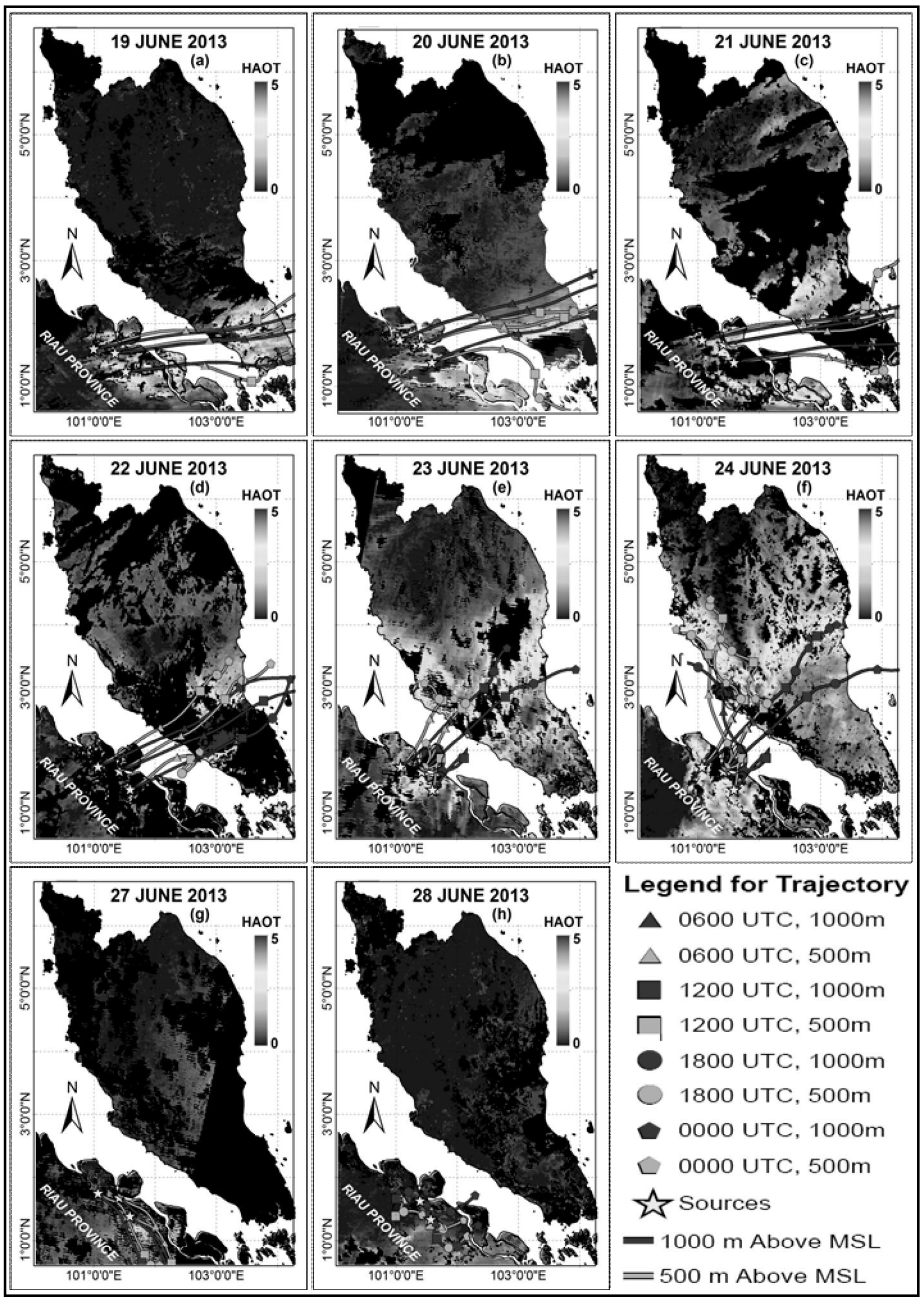


**Fig. 10** Spatial distribution of HAOT and its relationship with biomass burning aerosol induced haze transportation trajectories

The selected algorithm (Model-2) was used to retrieve HAOT (Fig. 10) for all the days from June 19 to 28, 2013. However, no HAOT map was produced for June 26 and 27 due to severe cloud contamination and missing MODIS data. The daily HAOT map of June 19, 2013 (Fig. 10a), shows a high concentration of aerosol ($1.0 < \text{HAOT} < 4$) mostly over parts of Riau Province (Sumatra), southern Malaysia (Johor and Malacca) and Singapore. Meteorological records (2013 Southeast Asian haze, 2013) indicate that thick biomass burning aerosol induced haze was observed mostly over the source areas of Sumatra. The haze was then transported to parts of Malaysia (Johor and Malacca) and Singapore by an unusually strong southwest monsoon (Vadrevu *et al.* 2014), resulting in API and PSI levels of 119–160 and 93–118 in Malaysia and Singapore, respectively. Transportation of biomass burning aerosol by the strong wind over these areas was also supported by forward trajectory analysis using HYSPLIT (Fig. 10a), which indicates that biomass burning aerosol was transported from the sources areas in Sumatra (Indonesia) to Singapore and part of Johor (Malaysia) within only 6 h.

The severity of the biomass burning aerosol induced haze increased on the following day, June 20 (Fig. 10b), as it was transported continuously by the strong southwest monsoon in the same direction and with similar speed as that on the previous day (Fig. 10b). The aerosol depicted by HAOT on June 20 (Fig. 10b) indicated high concentrations over Johor, Malacca, Sumatra, and Singapore. This was corroborated by local meteorological records showing that areas in Johor (API = 181–383), Malacca (API = 119–137) and Singapore (PSI = 232–291) (2013 Southeast Asian haze, 2013).

During the following two days, June 21and 22, large areas over the study site were contaminated by very thin clouds. Despite this problem, the HAOT maps (Fig. 10c and Fig. 10d) show that in addition to that in Singapore, Johor, and Malacca, the biomass burning aerosol induced haze began to move northward over Peninsular Malaysia. The transportation trajectories for these two days (Fig. 10c and Fig. 10d) also indicate that the haze was transported from the sources in a more northeasterly direction than that during the previous two days owing to a slight shift of the southwest monsoon. However, the wind speed was slowed rapidly on June 22 (Fig. 10d), and haze began to accumulate over the study areas, showing higher HAOT values (Fig. 10d). The HAOT maps agree with ground station data as well, which indicate that on June 21 and 22, in addition to Johor (API = 170–323), Malacca (API = 164–205), and Singapore (PSI = 225–290), which were severely polluted, other parts of Malaysia such as Seremban (API = 109–187) and Port Klang (API = 100–199) were also affected (2013 Southeast Asian haze, 2013).

The HAOT maps (Fig. 10e and Fig. 10f) for June 23 and 24 clearly revealed that besides Singapore, most of Peninsular Malaysia was covered by severe biomass burning aerosol induced haze. The aerosol transportation trajectories on those days (Fig. 10e and Fig. 10f), indicate a weaker southwestern monsoon that was directed more northwesterly, which caused high concentrations of biomass burning aerosol induced haze in the Kuala Lumpur, Selangor, and Perak areas. Although the trajectory on June 24 (Fig. 10f) moved away from Peninsular Malaysia, the biomass burning aerosol from the previous day lingered over Malacca and Negeri Sembilan due to the lack of wind movement and dry/wet depletion of aerosol and moved slowly upward toward the Klang area (Malaysia). During these two days, the highest API reading, 301, was observed in Klang Valley (Malaysia) on June 24 (2013 Southeast Asian haze, 2013). This study also indicated a high value (HAOT= 4.2; Fig. 10f) over Klang Valley, and medium values ($1 < \text{HAOT} < 4.0$) were found over other parts of Malaysia, Singapore, and Sumatra (Indonesia; Fig. 10f).

Lastly, the June 27 and 28 HAOT maps (Fig. 10g and Fig. 10h) indicate only a slight biomass burning aerosol induced haze over the entire Peninsular Malaysia and Singapore, and most HAOT values had fallen to $<1$, or near normal conditions. The average API over Peninsular Malaysia was only 55 on June 28 (2013 Southeast Asian haze, 2013), and Singapore's PSI was only 46 (2013 Southeast Asian haze, 2013). The aerosol transportation trajectories in Fig. 10g and Fig. 10h indicate that the wind was very calm and that the southwest monsoon began to withdraw on June 27 and 28. This caused in the trajectories from Sumatra to move away from Peninsular Malaysia and Singapore.

**Reducing the missing pixels of HAOT map by interpolation technique**

The spatial distribution of HAOT (Fig. 10) affected by cloud contamination was a major hindrance in this study; therefore, producing a HAOT map without missing pixels is practically impossible in the SEA region. Therefore, as a final attempt, this study also explored the possibility of using the interpolation technique to generate an HAOT map without missing pixels for each day using the efficient Penalized Least Squares Method (PLSM) (Garcia, 2010).

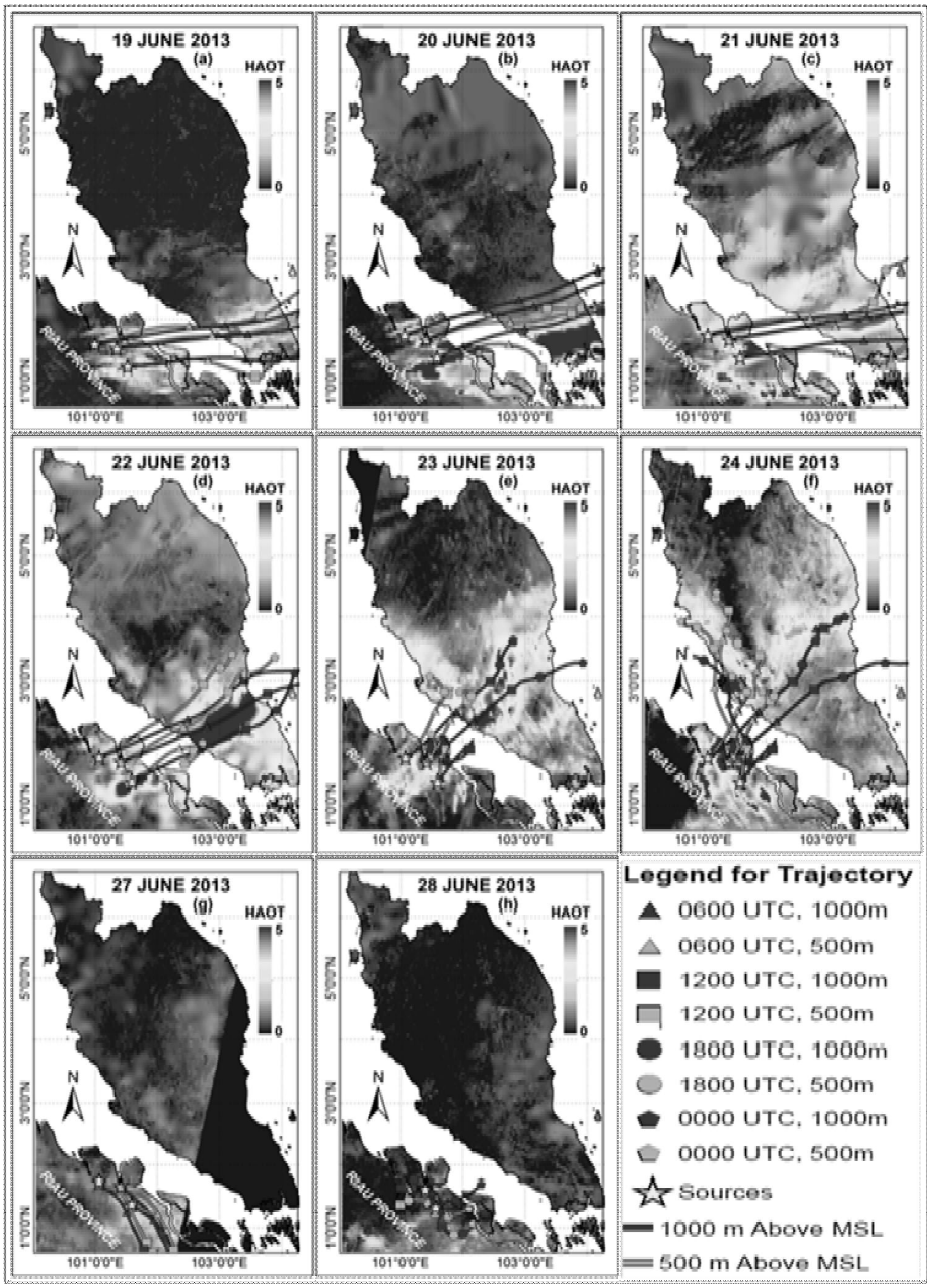


**Fig. 11** Interpolated daily HAOT maps without image mosaicking

During this step, filtering was applied to original HAOT maps to reduce artifacts from scatter and unwanted pixels. Different levels of iteration were investigated based on the extent of missing pixels and the severity of cloud contamination. From the interpolated daily HAOT maps (Fig. 11), we observed that it may be possible to generate useful HAOT maps without missing pixels for each day by using an interpolation technique. We also found that for a few days (Figs. 11a, 11b, and 11e–11h), interpolation techniques were able to reconstruct the missing pixels with relative ease because the cloud contamination was not very severe although small visual artifices were evident, particularly on June 20, 23, and 27 (Figs. 11b, 11e, and 11g).

For June 21, a satisfactory interpolated HAOT map without missing pixels was difficult to obtain owing to the very sporadic cloud contamination; however, the areas affected by the biomass burning aerosol induced haze can be observed more easily on the interpolated HAOT map (Fig. 11c) than on the original HAOT map (Fig. 10c). The interpolated HAOT map for June 22 (Fig. 11d) was reasonable, although some exaggeration of the HAOT values are visible in the upper and lower parts of the HAOT map owing to the severe data loss from cloud contamination in the original HAOT map (Fig. 10d). It is visually evident that these interpolated results (Fig. 11) are able to effectively portray the original HAOT distribution patterns (Fig. 10) without the problem of cloud contamination. The interpolated imagery shows the detailed spatial distribution of HAOT and helps to explain the movement of the aerosol induced haze pollution throughout the period.

**Discussion**

Despite the challenging nature of AOT retrieval in the SEA region, this study has developed an effective haze AOT retrieval algorithm. Theresults indicate that the developed model is highly successful considering the generated HAOT map at 500 m spatial resolution, validation results and trajectory analysis. The outcomes of this study agree with the results of other AOT retrieval studies (Wong *et al.* 2010; Li *et al.* 2013) that used similar methods although it is hardly possible to compare the obtained results with other studies owing to the differences in processing as well as validation techniques. Nevertheless, the results obtained in this study ($r^2$ = 0.80–0.90 between HAOT and AERONET; Fig. 7) are comparable with those of previous research (Li *et al.* 2013) that used MODIS data to obtain an accuracy of 0.82 ($r^2$) for the estimation of haze aerosol optical thickness due to severe particle pollution in China.

The high accuracy obtained from this study may be attributed to four factors. First, the use of a vector 6SV radiative transfer code to generate ρTOA_modeled reflectance that has the ability to consider radiation polarization effects, and use Mie code rather than the Henyey–Greenstein function for calculating the aerosol phase function (Kotchenova *et al.* 2006). Second, we used the MOD09GA MODIS surface reflectance product since this product is well validated and robust (Kotchenova and Vermote, 2007). Third, we used a robust cloud-screening process that combined thresholding and spatial variability techniques. Finally, we studied aerosol induced haze generated only from biomass burning and over less-heterogeneous land surfaces, both of which reduced the complexity of the radiative transfer code and produced consistent estimation parameters.

Moreover, the potential of the weekly (eight-day) averaging of surface reflectance versus a single date is quite clear; this outcome agrees with previous studies (Wong *et al.* 2010; Li *et al.* 2013) that used different types of surface reflectance averaging to minimize the uncertainty related to single-data imagery. The HYSPLIT forward trajectory analysis indicates that aerosol induced haze from Riau Province, Indonesia, moved from west to east toward other regions including Malaysia and Singapore on June 19–21generally within 12 h (Figs. 10a–10c). The observed aerosol induced haze movement is clearly in agreement with that reported by Vadrevu *et al.* (2014), who found similar patterns of aerosol induced haze movement for SEA pollution episode during June 2013 using remote sensing data. The proposed cloud-masking procedure creates less missing pixels in HAOT than that in the MODIS AOT product, which discards bright pixels with reflectance at 2.1 μm > 0.25 due to haze or clouds before applying the aerosol retrieval algorithm (Remer *et al.* 2005). However, the cloud masking procedure adopted in this paper is different but principally in agreement with several other studies **(**Remer *et al.* 2005) those employed threshold and spatial variability methods for cloud-mask generation from MODIS spectral bands.

Finally, we emphasize that the efforts involved in the image interpolation steps are worthwhile and effective for obtaining a better understanding of the spatial distribution of biomass burning aerosol induced haze. Although several limitations are present in the interpolated HAOT maps (Fig. 11), these interpolated outputs can convey much better and more effective information than the MODIS AOT product, which is limited by the severe missing pixels problem, or PSI and API point-based pollution estimation techniques that depend comprehensively on data interpolated from only a few points for spatial distribution of aerosol/pollution.

**Conclusions**

The proposed algorithm is in accordance with the necessity of the use of freely available satellite data for monitoring biomass burning aerosol induced haze monitoring in SEA that has long been advocated. This endeavor can be justified by the fact that the current monitoring system, largely based on measurements from a few ground-based stations, is inadequate to depict the spatial distribution of aerosol haze pollution induced by biomass burning in SEA. Despite the existence of several constraints, the developed model satisfactorily depicted the spatial distribution of biomass burning aerosol haze pollution. However, it is worthwhile to mention that this algorithm is developed following the general methodological considerations for aerosol retrieval from satellite data, therefore, it is possible to use this algorithm in other regions for haze or aerosol monitoring. But necessary adjustment for several parameters is required.

**Acknowledgements**
This research is supported by the Asia–Pacific Network for Global Change Research (APN, CAF2017-RR02-CMY-Siswanto) project. The authors express gratitude to Dr. Soo-Chin Liew and Dr. Santo V. Salinas Cortijo, the principal investigators of the Singapore AERONET station, and to Dr. Lim Hwee San at the USM_Penang AERONET station for providing the AERONET data. We also extend our gratitude to the National Environment Agency, Singapore, and the Department of Environment, Malaysia, for providing the PSI and API data, respectively.

## References

2013 Southeast Asian haze 2013. In Wikipedia, The Free Encyclopedia. Retrieved 10:58, March 17, 2015, fromhttps://en.wikipedia.org/wiki/2013_Southeast_Asian_haze#cite_note-hazegovsg-132.

Andreae MO and Merlet P 2001. Emission of trace gases and aerosols from biomass burning. *Global Biogeochem. Cycles*. doi:10.1029/2000GB001382

Arola A, Lindfors A, Natunen A and Lehtinen K 2007. A case study on biomass burning aerosols: effects on aerosol optical properties and surface radiation levels. Atmos. Chem. Phys., 7 , 4257-4266.Chander, G., Xiong, X., Choi, T., Angal, A., 2010. Monitoring on-orbit calibration stability of the Terra MODIS and Landsat 7 ETM+ sensors using pseudo-invariant test sites. *Remote Sens. Environ.* **114:** 925–939. doi: 10.1016/ j. rse. 2009.12.003

Chisholm RA, Wijedasa LS and Swinfield T 2016. The need for long-term remedies for Indonesia's forest fires. *Conserv. Biol.* doi:10.1111/cobi.12662

Dominick D, Juahir H, Latif MT, Zain SM and Aris AZ 2012. Spatial assessment of air quality patterns in Malaysia using multivariate analysis. *Atmos. Environ.* **60**: 172–181. doi:10.1016/ j.atmosenv.2012.06.021

Dreher J, Blottman PF, Sharp DW, Hoeth B and Van Speybroeck K 2009. *Configuring the HYSPLIT Model for National Weather Service Forecast Office and Spaceflight Meteorology Group Applications.* Contractor.

Duffie JA and Beckman WA 1994. *Solar Engineering of Thermal Processes*. 2nd Edn. pp. John Wiley, New York, U.S.A. 234-367.

Garcia D 2010. Robust smoothing of gridded data in one and higher dimensions with missing values. *Comput. Stat. Data Anal.* **54**: 1167–1178. doi:10.1016/j.csda.2009.09.020

Hsu NC, Tsay SC, King MD and Herman JR 2006. Deep Blue retrievals of Asian aerosol properties during ACE-Asia. *IEEE Trans. Geosci. Remote Sens.* **44**: 3180–3195. doi:10.1109/ TGRS. 2006. 879540

Kaskaoutis DG, Kharol SK, Sifakis N, Nastos PT, Sharma AR, Badarinath K and Kambezidis HD 2011. Satellite monitoring of the biomass-burning aerosols during the wildfires of August 2007 in Greece: climate implications. *Atmos. Environ.,* **45**: 716-726.

Kaufman YJ, Tanré D, Remer LA, Vermote EF, Chu A and Holben BN 1997. Operational remote sensing of tropospheric aerosol over land from EOS moderate resolution imaging spectroradiometer. *J. Geophys. Res. Atmos*. **102:** 17051–17067. doi:10.1029/96JD03988

Koe LCC, Arellano AF and McGregor JL 2001. Investigating the haze transport from 1997 biomass burning in Southeast Asia: Its impact upon Singapore. *Atmos. Environ*. **35:** 2723–2734. doi:10.1016/S1352-2310(00)00395-2

Kotchenova SY and Vermote EF 2007. Validation of a vector version of the 6S radiative transfer code for atmospheric correction of satellite data. Part II. Homogeneous Lambertian and anisotropic surfaces. *Appl. Opt.* **46**: 4455–4464. doi:10.1364/AO.46.004455

Kotchenova SY, Vermote EF, Matarrese R and Klemm FJ 2006. Validation of a vector version of the 6S radiative transfer code for atmospheric correction of satellite data. Part I: Path radiance. *Appl. Opt.* **45**: 6762–6774. doi:10.1364/AO.45.006762

Langmann B 2007. A model study of smoke-haze influence on clouds and warm precipitation formation in Indonesia 1997/1998. *Atmos. Environ*. **41**: 6838–6852. doi:10.1016/j. atmosenv. 2007.04.050

Lee KH, Kim YJ and Kim MJ 2006. Characteristics of aerosol observed during two severe haze events over Korea in June and October 2004. *Atmos. Environ*. **40**: 5146–5155. doi:10.1016 / j. atmosenv. 2006.03.050

Levy RC, Remer LA, Kleidman RG, Mattoo S, Ichoku C, Kahn R and Eck TF 2010. Global evaluation of the Collection 5 MODIS dark-target aerosol products over land. *Atmos. Chem. Phys.* **10**: 10399–10420. doi:10.5194/acp-10-10399-2010

Levy RC, Remer LA, Mattoo S, Vermote EF and Kaufman YJ 2007. Second-generation operational algorithm: Retrieval of aerosol properties over land from inversion of Moderate Resolution Imaging Spectroradiometer spectral reflectance. *J. Geophys. Res. Atmos.* **112**: doi:10.1029/2006JD007811

Li C, Lau AKH, Mao J and Chu DA 2005. Retrieval, validation, and application of the 1-km aerosol optical depth from MODIS measurements over Hong Kong, In: *IEEE Transactions on Geoscience and Remote Sensing*. pp. 2650–2658. doi:10.1109/TGRS.2005.856627

Li S, Chen L, Xiong X, Tao J, Su L, Han D and Liu Y 2013. Retrieval of the Haze Optical Thickness in North China Plain Using MODIS Data. *Geosci. Remote Sens., IEEE Trans*. **51**: 2528–2540. doi:10.1109/TGRS.2012.2214038

Lyapustin A, Wang Y, Laszlo I and Korkin S 2012. Improved cloud and snow screening in MAIAC aerosol retrievals using spectral and spatial analysis. *Atmos. Meas. Tech.* **5**: 843–850. doi:10.5194/amt-5-843-2012

Mahmud M 2009. Mesoscale model simulation of low level equatorial winds over Borneo during the haze episode of September 1997. *J. Earth Syst. Sci.* **118**: 295–307. doi:10.1007/s12040-009-0032-7

Nichol Janet 1998. Smoke haze in Southeast Asia: A predictable recurrence. *Atmos. Environ*. **32**: 2715–2716.

Radojevic M 1997. The Haze in Southeast Asia. *Environ. Sci.* **6:**1–3.

Reid JS, Hyer EJ, Johnson RS, Holben BN, Yokelson RJ, Zhang J, Campbell JR, Christopher SA, Di Girolamo L, Giglio L, Holz RE, Kearney C, Miettinen J, Reid EA, Turk FJ, Wang J, Xian P, Zhao G, Balasubramanian R, Chew BN, Janjai S, Lagrosas N, Lestari P, Lin NH, Mahmud M, Nguyen AX, Norris B, Oanh NTK, Oo M, Salinas SV, Welton EJ and Liew SC 2013. Observing and understanding the Southeast Asian aerosol system by remote sensing: An initial review and analysis for the Seven Southeast Asian Studies (7SEAS) program. *Atmos. Res.* **122**: 403–468. doi:10.1016/j. atmosres. 2012.06.005

Reid JS, Xian P, Hyer EJ, Flatau MK, Ramirez EM, Turk FJ, Sampson CR, Zhang C, Fukada EM and Maloney ED 2012. Multi-scale meteorological conceptual analysis of observed active fire hotspot activity and smoke optical depth in the Maritime Continent. *Atmos. Chem. Phys*. **12**: 2117–2147. doi:10.5194/acp-12-2117-201

Remer LA, Kaufman YJ, Tanré D, Mattoo S, Chu DA, Martins JV, Li RR, Ichoku C, Levy RC, Kleidman RG, Eck TF, Vermote E and Holben BN 2005. The MODIS Aerosol Algorithm, Products, and Validation. *J. Atmos. Sci.* **62**: 947–973. doi:10.1175/ JAS3385.1

Tian B, Waliser DE, Kahn RA, Li Q, Yung YL, Tyranowski T, Geogdzhayev IV, Mishchenko MI, Torres O and Smirnov A 2008. Does the Madden-Julian Oscillation influence aerosol variability? *J. Geophys. Res. Atmos.* **113**: doi:10.1029/ 2007JD009372

Vadrevu KP, Kristofer L, Louis G and Justice C 2014. Analysis of Southeast Asian pollution episode during June 2013 using satellite remote sensing datasets. *Environ. Pollut.* **195**: 245–256. doi:10.1016/j.envpol.2014.06.017

Vermote EF and Kotchenova S 2008. Atmospheric correction for the monitoring of land surfaces. *J. Geophys. Res.* **113**: D23S90. doi:10.1029/ 2007JD009662

von Hoyningen-Huene W, Kokhanovsky AA, Burrows JP, Bruniquel-Pinel V, Regner P and Baret F 2006. Simultaneous determination of aerosol- and surface characteristics from top-of-atmosphere reflectance using MERIS on board of ENVISAT. *Adv. Sp. Res.* **37**: 2172–2177. doi:10.1016/j.asr.2006.03.017

Wong MS, Lee KH, Nichol JE and Li Z 2010. Retrieval of Aerosol Optical Thickness Using MODIS 500 x 500 m2, a Study in Hong Kong and the Pearl River Delta Region. *IEEE Trans. Geosci. Remote Sens.* **48**: 3318–3327. doi:10.1109/ TGRS.2010.2045124

Xu C, Wang Z, Li S and Chen H 2012. A haze monitoring over North China Plain, in: International Geoscience and Remote Sensing Symposium (IGARSS). pp. 2474–2477. doi:10.1109/ IGARSS.2012.6350351

Zhang J and Reid JS 2006. MODIS aerosol product analysis for data assimilation: Assessment of over-ocean level 2 aerosol optical thickness retrievals. *J. Geophys. Res. Atmos.* **111**: doi:10.1029/ 2005JD00689